ARTICLE

P25-Graphene Composite as a High Performance Photocatalyst

Hao Zhang, Xiaojun Lv, Yueming Li, Ying Wang, and Jinghong Li*

Department of Chemistry, Key Laboratory of Bioorganic Phosphorus Chemistry & Chemical Biology, Tsinghua University, Beijing 100084, China

ABSTRACT Herein we obtained a chemically bonded TiO_2 (P25)-graphene nanocomposite photocatalyst with graphene oxide and P25, using a facile one-step hydrothermal method. During the hydrothermal reaction, both of the reduction of graphene oxide and loading of P25 were achieved. The as-prepared P25-graphene photocatalyst possessed great adsorptivity of dyes, extended light absorption range, and efficient charge separation properties simultaneously, which was rarely reported in other TiO_2—carbon photocatalysts. Hence, in the photodegradation of methylene blue, a significant enhancement in the reaction rate was observed with P25-graphene, compared to the bare P25 and P25-CNTs with the same carbon content. Overall, this work could provide new insights into the fabrication of a TiO_2—carbon composite as high performance photocatalysts and facilitate their application in the environmental protection issues.

KEYWORDS: graphene · P25-graphene · hydrothermal reduction · photocatalysis · chemical adsorptivity · extended light absorption · efficient charge separation

Photodegradation process of organic pollutants has attracted increasing attention during the past decades.[1] Among various strategies, TiO_2-based materials have been the most promising candidates for photocatalytic decontamination.[2] Particularly, the composites of TiO_2 and carbon (TiO_2—C) are currently being considered as potential photocatalysts in the purification of air and water.[3] The TiO_2—C composites can be generally categorized into three kinds: TiO_2-mounted activated carbon, carbon-doped TiO_2, and carbon-coated TiO_2, and each of them exhibits good photocatalytic activity.[4,5] However, several problems still hinder further promotion of efficiency of the present TiO_2—C composites, such as the marked decrease of the adsorptivity during photodegradation, the weakening of the light intensity arriving at catalysts' surface, and the lack of reproducibility due to the preparation and treatment variation, *etc.*[3,5] Therefore, it is of great significance to obtain a TiO_2—C composite possessing photocatalytic activity well beyond pure P25 with reproducibility and controllability, which could be potent in environment remediation.

Graphene is an atomic sheet of sp^2-bonded carbon atoms that are arranged into a honeycomb structure.[6] Apart from its unique electronic properties, the 2D planar structure material has several other excellent attributes, such as the large theoretical specific surface area[7] and the high transparency due to its one-atom thickness.[8] Moreover, the surface properties of graphene could be adjusted *via* chemical modification, which facilitates its use in composite materials.[9,10] Thus, the combination of TiO_2 and graphene is promising to simultaneously possess excellent adsorptivity, transparency, conductivity, and controllability, which could facilitate effective photodegradation of pollutants.

Herein we demonstrated a facile and reproducible route to obtain a chemically bonded TiO_2 (P25)-graphene composite (P25-GR) *via* a one-step hydrothermal reaction. In the as-prepared P25-GR photocatalyst, P25 nanoparticles were loaded on the platform of a graphene nanosheet, as illustrated in Scheme 1. Because of the unique properties of graphene, the composite simultaneously covered three excellent attributes: the increasing adsorptivity of pollutants, extended light absorption range, and facile charge transportation and separation, which were rarely reported in other TiO_2—C composites. In the photodegradation of methylene blue, P25-GR showed significant improvement compared to the bare P25. Moreover, in comparison to the P25-CNTs composite, which is a typical representative of TiO_2—C composites,[3] it also exhibited a higher photocatalytic activity. The enhancement of P25-GR over P25-CNTs was largely ascribed to its giant two-

*Address correspondence to jhli@mail.tsinghua.edu.cn.

Received for review September 14, 2009 and accepted December 22, 2009.

Published online December 30, 2009. 10.1021/nn901221k

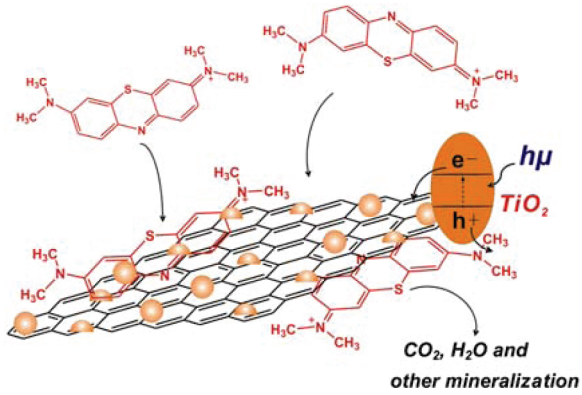

Scheme 1. Schematic structure of P25-GR and tentative processes of the photodegradation of methylene blue (MB) over P25-GR. P25 nanoparticles are dispersed on the graphene support, and the carbon platform plays important roles during the photodegradation of MB in three aspects: (i) Increase catalyst adsorptivity. MB molecules could transfer from the solution to the catalysts' surface and be adsorbed with offset face-to-face orientation *via* $\pi-\pi$ conjugation between MB and aromatic regions of the graphene, and therefore, the adsorptivity of dyes increases compared to bare P25. (ii) Extend light absorption. The chemical bonds of Ti−O−C and good transparency of graphene render a red shift in the photoresponding range and facilitate a more efficient utilization of light for the catalyst. (iii) Suppress charge recombination. Graphene could act as an acceptor of the photogenerated electrons by P25 and ensure fast charge transportation in view of its high conductivity, and therefore, an effective charge separation can be achieved.

dimensional planar structure favorable for dye adsorption and charge transportation. This high performance photocatalyst is anticipated to open new possibilities in the application of TiO_2−C composites as the photocatalysts in environment remediation.

RESULTS AND DISCUSSION

Characterizations of P25-GR. The exfoliated graphene oxide (GO) could be reduced to graphene *via* hydrothermal reaction with a small amount of residual groups as described in the literature.[11] Here we adopted a similar strategy in the fabrication of P25-graphene (denoted as P25-GR below, carbon content was *ca.* 1 wt %) with P25 and GO. In the reaction process, graphene oxide was reduced to graphene, simultaneously with the dispersion of P25 nanoparticles on the graphene sheet. Typical morphological, spectroscopic, and structural information of the as-prepared P25-GR is shown in Figure 1. The TEM results in Figure 1a were in line with the tentative structure of P25-GR illustrated in Scheme 1. The obtained composite retained the two-dimensional sheet structure with micrometers-long wrinkles after the hydrothermal reduction. Because of the distribution of carboxylic acid groups on the GO as discussed later, the P25 nanoparticles dispersed on the carbon support and were eager to accumulate along the wrinkles and edge. Figure 1b shows the FTIR spectra of P25 (curve 1), graphene obtained by hydrothermal reduction (curve 2), and the as-prepared P25-GR (curve 3). For P25-GR, the broad absorption at low frequency (below 1000 cm^{-1}) was attributed to the vibration of Ti−O−Ti bonds in TiO_2, similar to that in the spectrum of P25 (curve 1). The absorption band appearing at *ca.* 1600 cm^{-1} clearly showed the skeletal vibration of the graphene sheets, indicating the formation of graphene during the hydrothermal reaction.[11] This skeletal vibra-

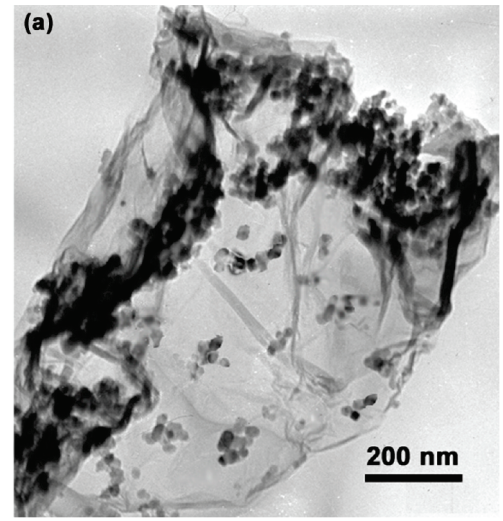

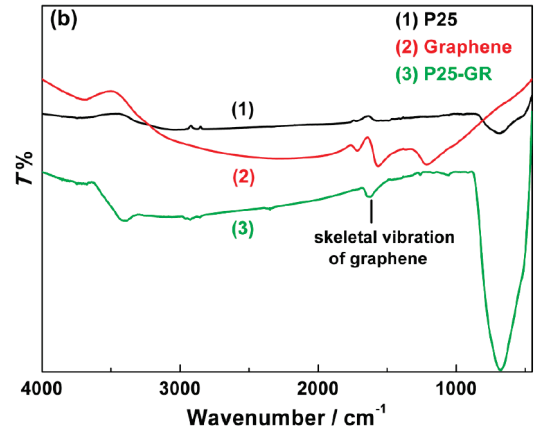

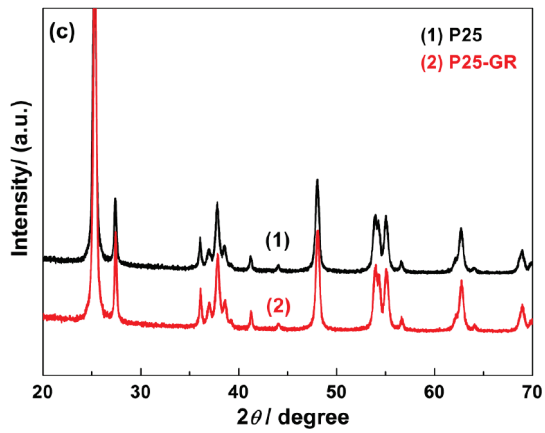

Figure 1. (a) Typical TEM image of P25-GR, with P25 loading on the surface of graphene and concentrating along the wrinkles. (b) Fourier transform infrared (FTIR) spectra of (1) P25, (2) graphene obtained by hydrothermal reduction, and (3) P25-GR in the range of 4000−450 cm^{-1}. (c) XRD patterns of (1) P25 and (2) P25-GR.

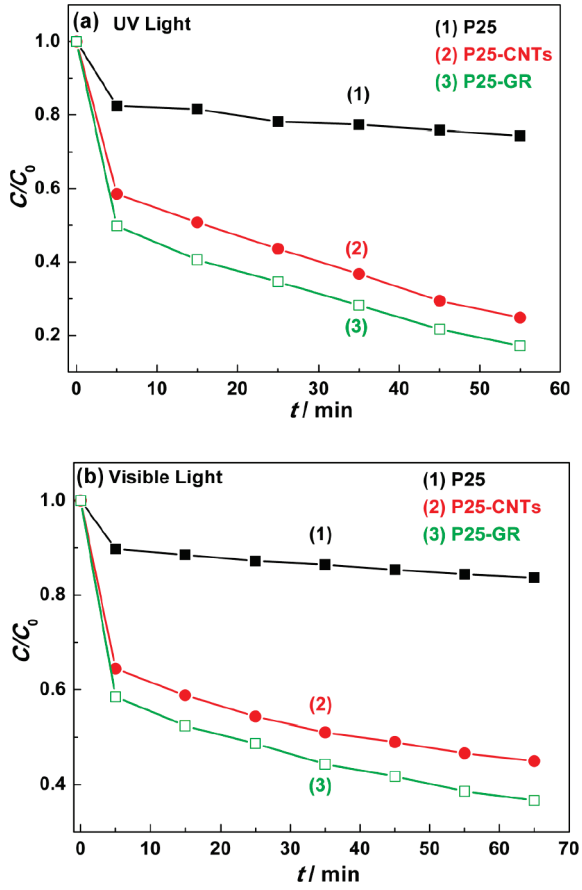

Figure 2. Photodegradation of methylene blue under (a) UV light and (b) visible light (λ > 400 nm) over (1) P25, (2) P25-CNTs, and (3) P25-GR photocatalysts, respectively.

tion peak was also observed in the FTIR spectrum of graphene prepared by hydrothermal reduction of GO (curve 2). Besides, in curve 2, the small peak around 1726 cm^{-1} was assigned to C═O stretching of the residual COOH groups. The above results confirmed the reduction of GO and the combination of P25 and graphene in the composite. Moreover, the chemical bonding between the two components in the composite could also be deduced. Pure P25 powder showed a low frequency band around 690 cm^{-1}, which corresponded to the vibration of Ti−O−Ti bonds. However, in the as-prepared P25-GR, the broad absorption below 1000 cm^{-1} was much plumper than the corresponding peak in pure P25 and shifted toward high wavenumber (Supporting Information Figure S1). In fact, this peak can be looked at as a combination of Ti−O−Ti vibration and Ti−O−C vibration (798 cm^{-1}).[12] The presence of Ti−O−C bonds indicated that, during the hydrothermal reduction, graphene oxide, with the residual carboxylic acid functional groups, firmly interacted with the surface hydroxyl groups of P25 nanoparticles and finally formed the chemically bonded P25-GR composites.[10] Because the carboxyl acid groups of GO were likely situated at the edge,[13] more P25 particles were observed along the edge and wrinkles than on the basal plane, as shown in Figure 1a. In addition, P25-GR showed similar XRD pattern with pure P25 (Figure 1c), and no diffraction peaks for carbon species were observed in the composite, which might be due to the low amount and relatively low diffraction intensity of graphene. Besides, for comparison in photocatalysis, we also prepared graphene *via* hydrothermal reduction of GO, and its structural and spectroscopic information is shown in Supporting Information Figure S2.

Photocatalytic Measurements. The photocatalytic activities of P25, P25-GR, and P25-CNTs (also prepared *via* hydrothermal method; see Methods section) were measured by the photodegradation of methylene blue (MB) as model reaction under UV and visible light (λ > 400 nm), and the results are shown in Figure 2a,b, respectively. The normalized temporal concentration changes (C/C_0) of MB during the photodegradation were proportional to the normalized maximum absorbance (A/A_0) and derived from the changes in the dye's absorption profile (λ = 660 nm) at a given time interval. It was clear from Figure 2 that the P25-GR composite showed significant progress in the photodegradation of MB compared to P25, and it also exhibited higher efficiency than P25-CNTs by *ca.* 20%. Under UV light irradiation, ~85 and ~70% of the initial dyes were decomposed by P25-GR and P25-CNTs after less than 1 h, respectively. Contrastingly, nearly 75% of the initial dye still remained in the solution after the same time period for bare P25. In addition, in the case of visible light photodegradation (Figure 2b), P25 showed rather poor photocatalytic activity due to its limited photoresponding range and only 12% of the initial contaminants diminished after more than 1 h, whereas the P25-GR composite photocatalyst showed remarkable improvements in the photodegradation rate where 65% of the dye molecules were decomposed after the same time period. The durability of the P25-GR catalyst for the degradation of MB under UV light was also checked (Figure S3). The photodegradation of MB was monitored for four consecutive cycles, each for 55 min. After each cycle, P25-GR was filtrated and washed thoroughly with water and fresh MB solution was added. There was no significant decrease in photodegradation rate during the four consecutive cycles, indicating the good stability of the prepared P25-GR photocatalyst. The high performance of P25-GR should be attributed to the following three properties.

Enhanced Adsorptivity. During the photocatalysis, three factors are crucial,[14] that is, the adsorption of contaminant molecules, the light absorption, and the charge transportation and separation, as illustrated by Scheme 1. The advancement of P25-GR in the photocatalysis should be first attributed to the enhanced adsorptivity, which is a prequisite for good photocatalytic activity.[15] P25-GR showed the best adsorption strength among the three catalysts (Figure 2) and the remaining concentration fraction of MB after dark adsorption (see experimental details in Methods) on the catalysts obtained

from UV−visible absorption spectra verified this assertion, as shown in Figure 3. It was obvious that, after equilibrium in the dark for 10 min, most dye molecules (*ca.* 90%) remained in the solution with bare P25 as the catalyst, whereas a large amount of dye molecules was adsorbed on the surface of P25-GR.

It is noteworthy that the reason for the enhanced adsorptivity of P25-GR was different from the traditional TiO_2-mounted activated carbon system, whose enhancement in the photocatalysis should be largely assigned to the great physical adsorption. There were no significant changes in the BET specific area (47.572, 54.226, and 51.034 $m^2\ g^{-1}$ for P25, P25-CNTs, and P25-GR, respectively) among the three catalysts, indicating that the adsorptivity should not merely originate from simple physical adsorption. Moreover, the enhanced adsorptivity should be largely assigned to the selective adsorption of the aromatic dye on the catalyst. Specifically, we suggested the adsorption was noncovalent and driven by the π−π stacking between MB and aromatic regions of the graphene, which was similar to the conjugation between aromatic molecules and CNTs.[16] In addition, the P25-GR showed better adsorption of MB than P25-CNTs mainly due to its giant π-conjugation system and two-dimensional planar structure, and thereby exhibited faster photodegradation of the dyes. On the basis of the above results, we proposed Scheme 1 for the photocatalysis process. MB molecules were adsorbed on the graphene surface with offset face-to-face orientation *via* π−π conjugation until adsorption−desorption equilibrium.[16] Under irradiation, the P25 particles were excited and the photogenerated carriers could easily transfer to the nearby MB and take part in the redox reactions. As the decomposition of dyes, the adsorption equilibrium broke and more MB would transfer from solution to the interface and subsequently be decomposed into CO_2, H_2O, and other mineralization through a series of redox reactions. Therefore, there would be a synergetic effect between adsorptivity and photoreactivity, and a coupling between adsorption and photocatalytical reaction could be achieved in a single process, resulting in an appreciable improvement in photodegradation of MB compared to bare P25 and P25-CNTs.

However, adsorption was not the only influential factor. First, without irradiation, the dye solution achieved adsorption equilibrium after 5−10 min, and more than 60% of the initial dye molecules still remained in the solution after 1 h (Supporting Information Figure S4a). Moreover, we tested the UV light photodegradation rate of MB over P25-graphene catalyst obtained by physical mixing of P25 and as prepared graphene (Figure S4b). In the mixture of P25 and graphene, the adsorptivity was enhanced while the chemical bonding between two components was not established. As a result, the physical mixture of P25 and graphene showed much poorer activity in the photodegradation compared to the prepared chemically bonded P25-GR. Accordingly, the chemical bonds play an important role in the photodegradation, and besides the adsorption of dyes, there must be other factors that contributed to the enhanced photoactivity.

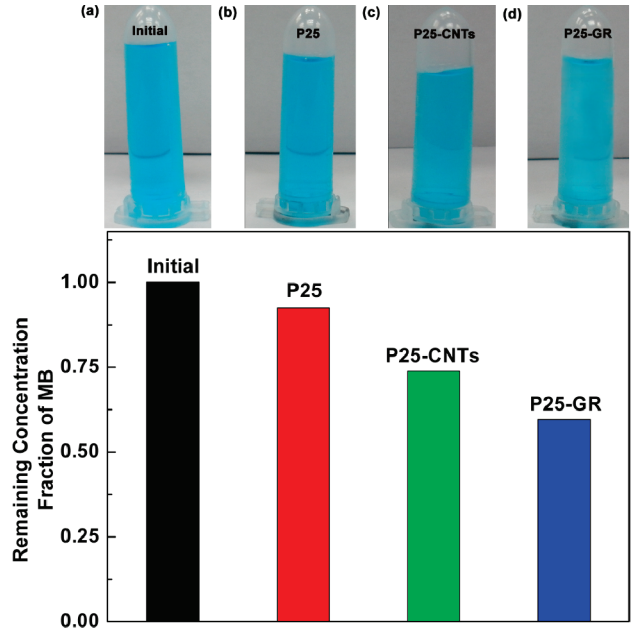

Figure 3. Bar plot showing the remaining methylene blue (MB) in solution: (a) initial and equilibrated with (b) P25, (c) P25-CNTs, and (d) P25-GR in the dark after 10 min stirring. Pictures of the corresponding dye solutions are on the top for each sample.

Extended Light Absorption Range. As mentioned above, the absorption range of light plays an important role in the photocatalysis, especially for the visible light photodegradation of contaminants. As shown in Figure 4, there was an obvious red shift of *ca.* 30−40 nm in the absorption edge of P25-GR powder, compared to bare P25. This result indicated that the narrowing of the band gap of P25 occurred with the graphene introduction. This narrowing should be attributed to the chemical bonding between P25 and GR, that is, the formation of Ti−O−C bond, similar to the case of carbon-doped TiO_2 composites.[12,17] As a result of the extended

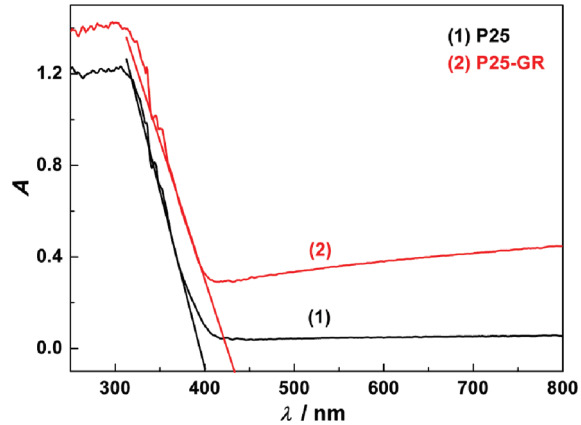

Figure 4. Diffuse reflectance absorption spectra of (1) P25 and (2) P25-GR.

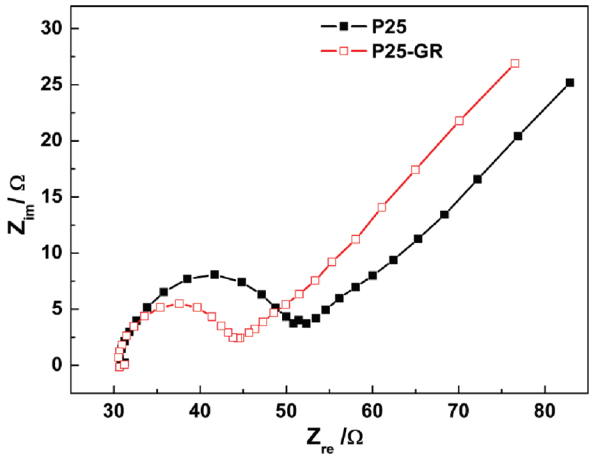

Figure 5. EIS changes of P25 (■) and P25-GR (□) electrodes. The EIS measurements were performed in the presence of a 2.5 mM $K_3[Fe(CN)_6]/K_4[Fe(CN)_6]$ (1:1) mixture as a redox probe in 0.1 M KCl aqueous solution.

photoresponding range of *ca.* 430−440 nm (corresponding to the violet-blue region in electromagnetic spectrum), a more efficient utilization of the solar spectrum could be achieved, and P25-GR showed significant improvement in the photodegradation of MB over bare P25, especially under visible light irradiation, as Figure 2 demonstrates. The visible light photoactivity of the P25-GR catalyst is expected to facilitate its use in practical environmental remediation.

Efficient Charge Separation and Transportation. Another important role of graphene in the P25-GR composite is the electron acceptor and transporter. On the one hand, graphene has been reported to be a competitive candidate for the acceptor material due to its two-dimensional π-conjugation structure,[18] and in the TiO_2-graphene system, the excited electrons of TiO_2 could transfer from the conduction band to graphene *via* a percolation mechanism.[19] Thus, in P25-GR, graphene served as an acceptor of the generated electrons of P25 and effectively suppressed the charge recombination, leaving more charge carriers to form reactive species and promote the degradation of dyes, as shown in Scheme 1. On the other hand, graphene has unexpectedly excellent conductivity due to its two-dimensional planar structure.[20] Therefore, the rapid transport of charge carriers could be achieved and an effective charge separation subsequently accomplished. As shown in Figure 5, the typical electrochemical impedance spectra were presented as Nyquist plots, and it is observed that, with the introduction of graphene, though in small amount, the semicircle in the plot became shorter, which indicated a decrease in the solid state interface layer resistance and the charge transfer resistance on the surface.[21] Overall, both the electron-accepting and transporting properties of graphene in the composite could contribute to the suppression of charge recombination, and thereby a higher rate in the photocatalysis would be achieved.

In conclusion, chemically bonded P25-GR photocatalyst with high performance has been successfully and directly produced *via* a one-step hydrothermal method. This composite possessed great adsorptivity of dyes, extended photoresponding range, and enhanced charge separation and transportation properties simultaneously. On the basis of these advantages, P25-GR demonstrated significant advancement over bare P25 in the photodegradation of MB dye under both UV and visible light irradiation. Moreover, it also showed higher photodegradation rate than the P25-CNTs, mainly due to its giant two-dimensional planar structure, which facilitated a better platform for adsorption of dyes and charge transportation. With further optimization of the parameters, such as the content of graphene in the composite and the control in preparation, the photoactivity of P25-GR is expected to be remarkably enhanced. This work is anticipated to open a new possibility in the investigation of TiO_2−C composites and promote their practical application in addressing various environmental issues.

METHODS

Reagents: Graphite powder (99.95%, 325 mesh) was purchased from Alfa Aesar. Multiwalled carbon nanotubes were from Tsinghua University.[22] The carbon nanotubes (CNTs) were produced by catalytic chemical vapor deposition method with an inner diameter of 3−5 nm, an outer diameter of 10 nm, and a length of more than several micrometers. Before used, the CNTs were purified by refluxing in nitric acid solutions for 12 h. TiO_2 (P25, 20% rutile and 80% anatase) was purchased from Degussa. Unless otherwise specified, methylene blue (MB) and other reagents and materials involved were obtained commercially from the Beijing Chemical Reagent Plant (Beijing, China) and used as received without further purification. Ultrapure water (resistivity ≥18 MΩ cm) was used during the experimental process. The experiments were carried out at room temperature and humidity.

Synthesis of P25-Graphene Composite: First, graphene oxide (GO) was synthesized by the modified Hummers' method.[23,24] In detail, 3 g of graphite was put into a mixture of 12 mL of concentrated H_2SO_4, 2.5 g of $K_2S_2O_8$, and 2.5 g of P_2O_5. The solution was heated to 80 °C and kept stirring for 5 h in an oil bath. Then the mixture was diluted with 500 mL of deionized water, and the product was obtained by filtering using 0.2 μm Nylon film and dried under ambient condition. Thereafter, the product was reoxidized by Hummers and Offeman methods to produce the graphite oxide.[24] After the exfoliation by sonicating 0.1 mg/mL of graphite oxide dispersion for 1 h, the graphene oxide was recovered by filtration and vacuum drying.

The P25-graphene composite (P25-GR) was obtained *via* a hydrothermal method based on Rajamathi's work with modifications.[11] Briefly, 2 mg of GO was dissolved in a solution of distilled H_2O (20 mL) and ethanol (10 mL) by ultrasonic treatment for 1 h, and 0.2 g of P25 was added to the obtained GO solution and stirred for another 2 h to get a homogeneous suspension. The suspension was then placed in a 40 mL Teflon-sealed autoclave and maintained at 120 °C for 3 h to simultaneously achieve the reduction of GO and the deposition of P25 on the carbon substrate. Finally, the resulting composite was recovered by fil-

tration, rinsed by deionized water several times, and dried at room temperature. For comparison, blank graphene or P25-CNTs (with the same the content of carbon, 1 wt %) were obtained by reducing GO *via* hydrothermal route under the same condition but without the addition of P25 or replacing GO with CNTs.

Characterization: Transmission electron microscopy (TEM) images were taken with a JEOL JEM-1010 transmission electron microscope operated at 120 kV. Fourier transform infrared (FTIR) spectra were carried out using Perkin-Elmer spectrometer in the frequency range of 4000−450 cm^{-1} with a resolution of 4 cm^{-1}. Diffuse reflectance spectra (DRS) of P25 and P25-GR powders were recorded in the range from 250 to 800 nm using a Hitachi U-3010 spectroscope and $BaSO_4$ was used as a reference. Powder X-ray diffraction (XRD) was performed on a Bruker D8-Advance X-ray diffractometer with monochromatized Cu Kα radiation (λ = 1.5418 Å). Specific surface areas of the catalysts were measured at 77 K by Brunauer−Emmett−Teller (BET) nitrogen adsorption−desorption (Micromeritics ASAP 2010 Instrument).

Photocatalytic Experiments: The photodegradation of methylene blue (MB) dyes was observed based on the absorption spectroscopic technique. In a typical process, aqueous solution of the MB dyes (0.01 g/L, *i.e.*, 2.7 × 10^{-5} M, 40 mL) and the photocatalysts (P25/P25-GR/P25-CNTs, 30 mg) were placed in a 50 mL cylindrical quartz vessel. Under ambient conditions and stirring, the photoreaction vessel was exposed to the UV irradiation produced by a 100 W high pressure Hg lamp with the main wave crest at 365 nm, which was positioned 30 cm away from the vessel (intensity at wavelength of 365 nm at the catalyst mixture surface was 30 μW/cm^2, estimated with a radiometer, Photoelectronic Instrument Co. IPAS). The photocatalytic reaction was started by turning on the Hg lamp, and during the photocatalysis, all other lights were insulated. At given time intervals, the photoreacted solution was analyzed by recording variations of the absorption band maximum (660 nm) in the UV−visible spectra of MB, using a UV−visible spectrophotometer (UV 2100, Shimadzu). In the visible light photocatalysis, a similar procedure was constructed with a 500 W xenon lamp and a cutoff filter equipped as the light source (λ > 400 nm, intensity at wavelength of 420 nm at the catalyst mixture surface was 2000 μW/cm^2, estimated with a radiometer, Photoelectronic Instrument Co. IPAS). During the photodegradation, the temperature was kept at 20−25 °C and the pH of the dispersion was kept at 6. In the durability test of P25-GR catalyst in the photodegradation of MB under UV light, four consecutive cycles were tested. At the beginning, 30 mg of P25-GR was dispersed in 40 mL of MB solution (2.7 × 10^{-5} M). Then the mixture underwent four consecutive cycles, each lasting for 55 min. After each cycle, the catalyst was filtrated and washed thoroughly with water, and then fresh MB solution (2.7 × 10^{-5} M) was added to the catalyst. Dark adsorption test was adopted to compare the adsorptivity of P25, P25-GR, and P25-CNTs. In this test, 30 mg of catalyst (P25, P25-GR, or P25-CNTs) was dispersed in 40 mL of MB solution (2.7 × 10^{-5} M) with stirring and kept in the dark for 10 min. Then the dispersion was centrifuged and the MB solution was taken to the UV−visible absorption measurement. From the difference in the absorbance before and after adsorption, the amount of dyes adsorbed by the catalyst could be estimated.

Fabrication of Film Electrodes and Electrochemical Impedance Spectra (EIS) Measurements: For the EIS measurement, P25 and P25-GR powders were fabricated as the film electrodes by the method reported in our previous work.[25] First, the powders and ethanol were mixed homogeneously (150 mg/mL), and the obtained paste was then spread on the conducting fluorine-doped SnO_2 glass substrate (FTO, 15 Ω/square) with a glass rod, using adhesive tapes as spacers. Finally, the resultant films with a *ca.* 4 μm thickness and 1 cm^2 active area were calcinated at 450 °C for 2 h in N_2 atmosphere to achieve good electronic contact between the particles.

The EIS measurements were carried out on a PARSTAT 2273 potentiostat/galvanostat (Advanced Measurement Technology Inc., USA) by using three-electrode cells. The resultant electrode served as the working electrode, with a platinum wire as the counter electrode and a Ag/AgCl (saturated KCl) electrode as the reference electrodes, which was performed in the presence of a 2.5 mM $K_3[Fe(CN)_6]/K_4[Fe(CN)_6]$ (1:1) mixture as a redox probe in 0.1 M KCl solution. The impedance spectra were recorded with the help of ZPlot/ZView software under an ac perturbation signal of 5 mV over the frequency range of 1 MHz to 100 mHz.

Acknowledgment. This work was financially supported by the National Natural Science Foundation of China (No. 20975060) and National Basic Research Program of China (No. 2007CB310500).

Supporting Information Available: FTIR spectra of P25 and P25-GR with different magnifications, characterization of graphene prepared *via* hydrothermal method, durability and control experiments in photocatalysis, and some expanded discussion. This material is available free of charge *via* the Internet at http://pubs.acs.org.

REFERENCES AND NOTES

1. Hoffmann, M. R.; Martin, S. T.; Choi, W. Y.; Bahnemannt, D. W. Environmental Applications of Semiconductor Photocatalysis. *Chem. Rev.* **1995**, *95*, 69.
2. Rajeshwara, K.; Osugib, M. E.; Chanmaneec, W.; Chenthamarakshana, C. R.; Zanonib, M. V. B.; Kajitvichyanukuld, P.; Krishnan-Ayera, R. Heterogeneous Photocatalytic Treatment of Organic Dyes in Air and Aqueous Media. *J. Photochem. Photobiol. C* **2008**, *9*, 15.
3. Woan, K.; Pyrgiotakis, G.; Sigmund, W. Photocatalytic Carbon-Nanotube−TiO_2 Composites. *Adv. Mater.* **2009**, *21*, 2233.
4. Yang, L. X.; Luo, S. L.; Liu, S. H.; Cai, Q. Y. Graphitized Carbon Nanotubes Formed in TiO_2 Nanotube Arrays: A Novel Functional Material with Tube-in-Tube Nanostructure. *J. Phys. Chem. C* **2008**, *112*, 8939.
5. Inagaki, M.; Kojin, F.; Tryba, B.; Toyoda, M. Carbon Coated Anatase: The Role of the Carbon Layer for Photocatalytic Performance. *Carbon* **2005**, *43*, 1652.
6. Ishigami, M; Chen, J. H.; Cullen, W. G.; Fuhrer, M. S.; Williams, E. D. Atomic Structure of Graphene on SiO_2. *Nano Lett.* **2007**, *7*, 1643.
7. McAllister, M. J.; Li, J. L.; Adamson, D. H.; Schniepp, H. C.; Abdala, A. A.; Liu, J.; Herrera-Alonso, M.; Milius, D. L.; Car, R.; Prud'homme, R. K.; Aksay, I. A. Single Sheet Functionalized Graphene by Oxidation and Thermal Expansion of Graphite. *Chem. Mater.* **2007**, *19*, 4396.
8. Nair, R. R.; Blake, P.; Grigorenko, A. N.; Novoselov, K. S.; Booth, T. J.; Stauber, T.; Peres, N. M. R.; Geim, A. K. Fine Structure Constant Defines Visual Transparency of Graphene. *Science* **2008**, *320*, 1308.
9. Bekyarova, E.; Itkis, M. E.; Ramesh, P.; Berger, C.; Sprinkle, M.; de Heer, W. A.; Haddon, R. C. Chemical Modification of Epitaxial Graphene: Spontaneous Grafting of Aryl Groups. *J. Am. Chem. Soc.* **2009**, *131*, 1336.
10. Williams, G.; Seger, B.; Kamat, P. V. TiO_2-Graphene Nanocomposites. UV-Assisted Photocatalytic Reduction of Graphene Oxide. *ACS Nano* **2008**, *2*, 1487.
11. Nethravathi, C.; Rajamathi, M. Chemically Modified Graphene Sheets Produced by the Solvothermal Reduction of Colloidal Dispersions of Graphite Oxide. *Carbon* **2008**, *46*, 1994.
12. Sakthive, S.; Kisch, H. Daylight Photocatalysis by Carbon-Modified Titanium Dioxide. *Angew. Chem., Int. Ed.* **2003**, *42*, 4908.
13. Park, S; Lee, K. S.; Bozoklu, G.; Cai, W. W.; Nguyen, S. T.; Ruoff, R. S. Graphene Oxide Papers Modified by Divalent Ions-Enhancing Mechanical Properties *via* Chemical Cross-Linking. *ACS Nano* **2008**, *2*, 572.
14. Zhang, L. W.; Fu, H. B.; Zhu, Y. F. Efficient TiO_2 Photocatalysts from Surface Hybridization of TiO_2 Particles with Graphite-like Carbon. *Adv. Funct. Mater.* **2008**, *18*, 2180.
15. Morales, W.; Cason, M.; Aina, O.; de Tacconi, N. R.; Rajeshwar, K. Combustion Synthesis and Characterization of Nanocrystalline WO_3. *J. Am. Chem. Soc.* **2008**, *130*, 6318.

16. Liu, Z.; Robinson, J. T.; Sun, X. M.; Dai, H. J. PEGylated Nanographene Oxide for Delivery of Water-Insoluble Cancer Drugs. *J. Am. Chem. Soc.* **2008**, *130*, 10876.
17. Ren, W. J.; Ai, Z. H.; Jia, F. L.; Zhang, L. Z.; Fan, X. X.; Zou, Z. G. Low Temperature Preparation and Visible Light Photocatalytic Activity of Mesoporous Carbon-Doped Crystalline TiO_2. *Appl. Catal. B* **2007**, *69*, 138.
18. Liu, Q.; Liu, Z. F.; Zhang, X. Y.; Yang, L. Y.; Zhang, N.; Pan, G. L.; Yin, S. G.; Chen, Y. S.; Wei, J. Polymer Photovotaic Cells Based on Solution-Processable Graphene and P3HT. *Adv. Funct. Mater.* **2009**, *19*, 894.
19. Wang, X.; Zhi, L. J.; Müllen, K. Transparent, Conductive Graphene Electrodes for Dye-Sensitized Solar Cells. *Nano Lett.* **2008**, *8*, 323.
20. Novoselov, K. S.; Geim, A. K.; Morozov, S. V.; Jiang, D.; Zhang, Y.; Dubonos, S. V.; Grigorieva, I. V.; Firsov, A. A. Electric Field Effect in Atomically Thin Carbon Films. *Science* **2004**, *306*, 666.
21. He, B. L.; Dong, B.; Li, H. L. Preparation and Electrochemical Properties of Ag-Modified TiO_2 Nanotube Anode Material for Lithium-Ion Battery. *Electrochem. Commun.* **2007**, *9*, 425.
22. Wang, Y.; Wei, F.; Luo, G.; Yu, H.; Gu, G. The Large-Scale Production of Carbon Nanotubes in a Nano-agglomerate Fluidized-Bed Reactor. *Chem. Phys. Lett.* **2002**, *364*, 568.
23. Hummers, W. S.; Offeman, R. E. Preparation of Graphitic Oxide. *J. Am. Chem. Soc.* **1958**, *80*, 1339.
24. Wang, Y.; Li, Y. M.; Tang, L. H.; Lu, J.; Li, J. H. Application of Graphene-Modified Electrode for Selective Detection of Dopamine. *Electrochem. Commun.* **2009**, *11*, 889.
25. Zhang, H.; Wang, G.; Chen, D.; Lv, X. J.; Li, J. H. Tuning Photoelectrochemical Performances of $Ag-TiO_2$ Nanocomposites *via* Reduction/Oxidation of Ag. *Chem. Mater.* **2008**, *20*, 6543.